A&A 436, 687–695 (2005)
DOI: 10.1051/0004-6361:20042290

Astronomy & Astrophysics

A non-LTE analysis of the spectra of two narrow lined main sequence stars in the SMC⋆

I. Hunter[1], P. L. Dufton[1], R. S. I. Ryans[1], D. J. Lennon[2], W. R. J. Rolleston[1], I. Hubeny[3], and T. Lanz[4]

[1] APS Division, Department of Pure & Applied Physics, The Queen's University of Belfast, BT7 1NN, Northern Ireland, UK
e-mail: I.Hunter@qub.ac.uk
[2] Isaac Newton Group of Telescopes, Apartado de Correos 368, 38700 Santa Cruz de La Palma, Canary Islands, Spain
[3] Steward Observatory, University of Arizona, Tucson, AZ 85712, USA
[4] Department of Astronomy, University of Maryland, College Park, MD 20742, USA

Received 1 November 2004 / Accepted 20 February 2005

Abstract. An analysis of high-resolution VLT/UVES spectra of two B-type main sequence stars, NGC 346-11 and AV 304, in the Small Magellanic Cloud (SMC), has been undertaken, using the non-LTE TLUSTY model atmospheres to derive the stellar parameters and chemical compositions of each star. The chemical compositions of the two stars are in reasonable agreement. Moreover, our stellar analysis agrees well with earlier analyses of H II regions. The results derived here should be representative of the current base-line chemical composition of the SMC interstellar medium as derived from B-type stars.

Key words. stars: abundances – stars: atmospheres – stars: early-type – galaxies: individual: Small Magellanic Cloud

1. Introduction

The Magellanic Clouds have been intensively studied in terms of, for example, their star formation history (see, for example, Yoshizawa & Noguchi 2003; Harris & Zaritsky 2004; Zaritsky et al. 2004), kinematics (see, for example, Stanimirovic et al. 2004; Kim et al. 2003; Gardiner & Noguchi 1996), stellar populations (see, for example, Cioni & Habing 2003; Evans et al. 2004; Kunkel et al. 1995) and chemical compositions (see, for example, the reviews of Garnett 1999; and Westerlund 1997). This interest arises from their relative proximity (Harries et al. 2003), which means that it is possible to study individual stars and nebulae in detail. Additionally their relatively low extinction allows them to be viewed in their entirety. Their very different environments to that of our own Galaxy then makes them ideal for studying both stellar and galactic evolution.

In the case of mapping the chemical compositions of the Magellanic Clouds, a variety of targets have been studied including H II regions (see, for example, Russell & Dopita 1992; Garnett 1999; Kurt et al. 1999), the interstellar medium, ISM (Welty et al. 1997, 1999), early-type (Bouret et al. 2003; Korn et al. 2000, 2002; Rolleston et al. 2003; Trundle et al. 2004) and late-type (Barbuy et al. 1991; Spite et al. 1989, 1991; Hill 1997, 1999) stars. All these methods have particular strengths and limitations that can be characterised under two main headings. Firstly there is the physical model used in predicting the observed spectra. This model will make assumptions about the geometry of and physical conditions in the plasma and about the transfer of radiation, which will impact on the reliability of the derived chemical compositions. Equally important is the nature of the plasma that is observed. For example, ISM studies normally observe only the gas phase component, whilst the chemical compositions of stellar atmospheres may have been modified by mixing of nucleosynthetic material to the surface. The latter is particularly important as even relative unevolved B-type giants (Lennon et al. 2003; Korn et al. 2000) and O-type dwarfs (Bouret et al. 2003) appear to have contaminated atmospheres.

Such effects can be used to understand the physical processes that are occuring, e.g. the chemical composition and nature of ISM grains and the detail of how stars evolve. However these limit the usefulness of such techniques in estimating the current chemical composition of the interstellar medium in the host galaxy. Historically H II regions have been used for such studies as they directly sample the ISM and their emission line spectra are relatively easy to observe. Recent SMC studies show relatively good agreeement (see, for example, Russell & Dopita 1992; Reyes 1999; Garnett 1999; Kurt et al. 1999; Peimbert et al. 2000; and Testor 2001), illustrating the utility of the method and indirectly implying that the SMC is relatively well mixed. However, it is important that other methods are available both to investigate the possibility of systematic errors and also to extend the range of elements that can be studied. The spectra of main sequence B-type stars offer such an alternative as their atmospheres should be uncontaminated and indeed Korn et al. (2002) have studied such objects in the LMC. Additionally two narrow lined B-type stars, AV 304 and NGC 346-11 have been identified in the SMC and analysed by

⋆ Table 1 is only available in electronic form at
http://www.edpsciences.org

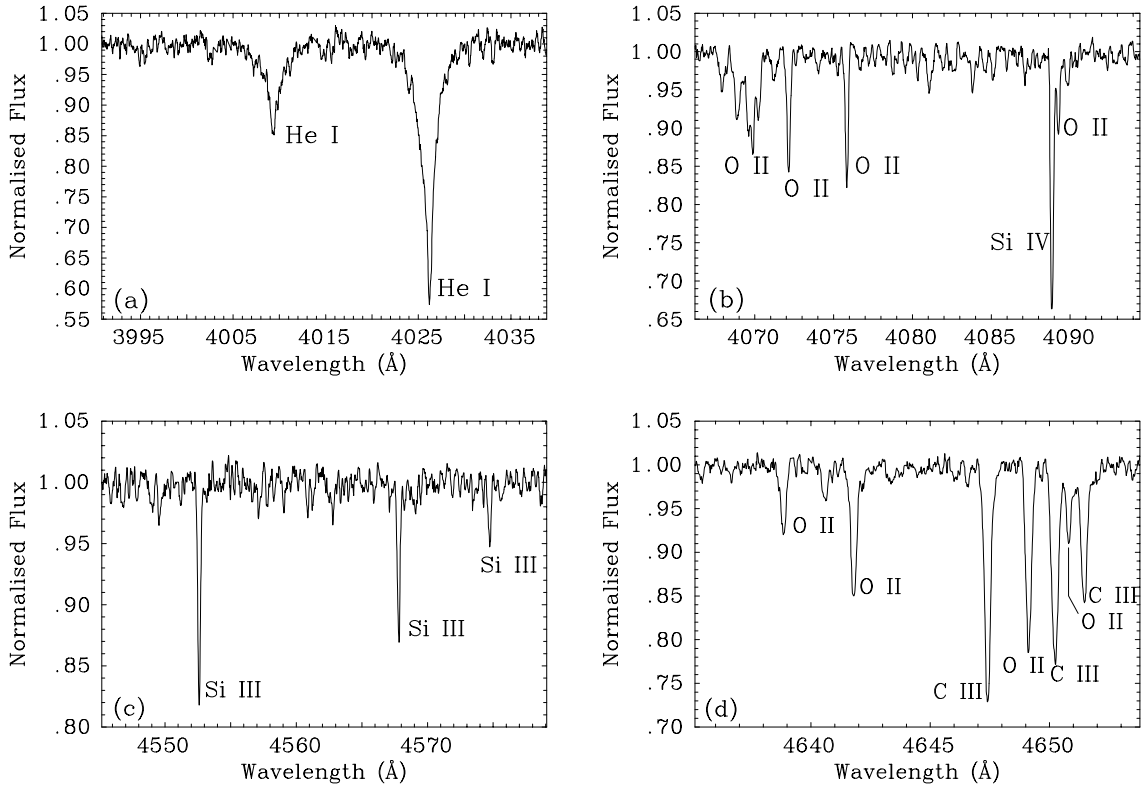

Fig. 1. Examples of the observed spectra of NGC 346-11 from UVES. These sample spectral regions include important lines such as Si IV **b)**, Si III **c)** and C III **d)**. Notice the lack of an obvious N II line at 3995 Å in **a)**.

Dufton et al. (1990) and Rolleston et al. (1993, 2003). These analyses were limited by their adoption of an LTE model atmosphere approach and for the two earlier analyses, by the moderate quality of the spectroscopic data for these relatively faint targets. Here we present non-LTE analyses of these two targets based on high quality UVES/VLT observations that should complement the existing H II region SMC studies.

2. Observations and data reductions

High-resolution spectra have been obtained for both NGC 346-11 and AV 304 using the Ultraviolet and Visual Echelle Spectrograph, UVES, (D'Odorico et al. 2000) on the UT2 (Kueyen) telescope at the European Southern Observatory. NGC 346-11 was observed during a three night run in November 2001, whilst the observations of AV 304, taken during a two night run in January 2001, have been previously discussed by Rolleston et al. (2003). UVES was operated using a two arm cross-disperser with CCD-44 chips, with slit widths of 1.5 arcsec and 1.0 arcsec for NGC 346-11 and AV 304 respectively. Complete spectral coverage in the range 3770–4980 Å was obtained for both stars and the echellograms were reduced to a one dimensional format using UVES pipe-line software. Combining the individual exposures resulted in signal-to-noise ratios of approximately 100 and 80 for NGC 346-11 and AV 304 respectively. Examples of sample regions of the observed spectra for NGC 346-11 and AV 304 are displayed in Fig. 1 and Rolleston et al. (2003) respectively. These spectral regions clearly show the high resolution and signal-to-noise ratio of our data.

For the NGC 346-11 spectrum, data reduction followed the procedures discussed by Rolleston et al. (2003). The spectrum analysis package DIPSO (Howarth et al. 1994) was used to normalise and then radial velocity correct the spectra. Equivalent widths were measured for all the observable absorption metal lines by non-linear least squares fitting using Gaussian profiles and a low order polynomial to represent the continuum. For well observed isolated features, an error estimate of normally less than 10% was found for the equivalent width measurements, whilst this increased to typically 20% for blended or weak absorption lines. The equivalent width estimates for both targets are listed in Table 1 available at the CDS. Table 1 contains the following information; Col. 1 lists the species of the observed spectral line, Col. 2 lists the rest wavelength of the observed line, Col. 3 lists the equivalent width of the observed lines in AV 304, Col. 4 lists the abundances derived from the equivalent widths and atmospheric paramters of AV 304, Col. 5 lists the equivalent width of the observed lines in NGC 346-11 and Col. 6 lists the abundances derived from the equivalent widths and atmospheric paramters of NGC 346-11.

3. Analysis

3.1. Non-LTE atmosphere calculations

The analysis is based on grids of non-LTE model atmospheres calculated using the codes TLUSTY and SYNSPEC (Hubeny 1988; Hubeny & Lanz 1995; Hubeny et al. 1998). Details of

the methods can be found in Ryans et al. (2003), while the grids have been discussed in more detail by Dufton et al. (2005) and hence we will limit ourselves to a short overview of the methods.

Briefly four grids have been generated with base metallicities corresponding to our Galaxy ($[\frac{\mathrm{Fe}}{\mathrm{H}}] = 7.5$ dex) and with metallicities reduced by 0.3, 0.6 and 1.1 dex. These lower metallicities were chosen so as to be representative of the LMC, SMC and low metallicity material. For each base metallicity, approximately 3000 models have been calculated covering a range of effective temperature from 12 000 to 35 000 K, logarithmic gravities (in cm s^{-2}) from 4.5 dex down to close to the Eddington limit (which will depend on the effective temperature) and microturbulences of 0, 5, 10, 20 and 30 km s^{-1}. Then for any set of atmospheric parameters, five full independent models were calculated keeping the iron abundance fixed but allowing the abundances of the light elements, C, N, O, Mg, Si and S, to vary from +0.8 dex to −0.8 dex around their base values. Effectively this approaches assumes that the line blanketing and atmospheric structure is dominated by iron and hence that the light element abundances can be varied without significantly affecting this structure. Tests discussed in Dufton et al. (2005) appear to confirm that this approach is reasonable.

These models are then used to calculate spectra, which in turn provide theoretical hydrogen and helium line profiles and equivalent widths for light metals for a range of abundances. The theoretical equivalent widths are then available via a GUI interface written in IDL, which allows the user to interpolate in order to calculate equivalent widths and/or abundance estimates for approximately 200 metal lines for any given set of atmospheric parameters. Ryans et al. (2003) reported that the increments of 0.4 dex used in our grids were fine enough to ensure that no significant errors were introduced by the interpolation procedures. Full theoretical spectra are also available for any given model. Details of the model atmosphere grids, atomic data used in the line strength calculations and wavelength ranges used in the equivalent width calculations are discussed in Dufton et al. (2005) and details are also avaliable at `http://star.pst.qub.ac.uk/`.

3.2. Stellar atmospheric parameters

Four parameters define the basic characteristics of the stellar atmosphere – effective temperature (T_{eff}), logarithmic gravity ($\log g$), mircoturbulence (ξ), and the metallicity (iron content) of the star. As these parameters are all inter-related, one must use an iterative process but by careful selection of the initial estimates, in most cases only two or three iterations were necessary. Standard techniques were used and as they have previously been discussed by, for example, Kilian (1992), Kilian et al. (1994), McErlean et al. (1999), Korn et al. (2000) and Trundle et al. (2004), they will only be briefly discussed here. Note that the grid of models with an iron abundance of 6.9 dex was initially used to determine the other parameters and the effect of varying this value will be discussed below.

Table 2. The stellar parameters and absolute abundance estimates, together with their estimated uncertainties, for NGC 346-11 and AV 304. The quantities inside brackets are the number of lines used to estimate the abundances. For the ions denoted with a * the abundance estimates have been calculated using LTE rather than non-LTE methods as discussed in Sect. 3.4.

	NGC 346-11			AV 304		
T_{eff} (K)	32 500	±1000		27 500	±1000	
$\log g$ (dex)	4.25	±0.20		3.90	±0.20	
ξ (km s^{-1})	5	±5		3	±3	
Spectral Type	B0V			B0.5V		
C II	7.45	±0.29	(2)	7.36	±0.12	(3)
C III	7.44	±0.18	(2)	7.66	±0.30	(2)
N II	6.73	±0.31	(1)	6.55	±0.18	(1)
O II	7.82	±0.20	(22)	8.13	±0.10	(42)
Mg II	6.77	±0.23	(1)	6.77	±0.16	(1)
Si III	6.42	±0.25	(3)	6.76	±0.19	(4)
Si IV	6.39	±0.27	(3)	6.73	±0.44	(2)
Ne II*	–	–		7.84	±0.16	(2)
Al III*	–	–		5.33	±0.11	(1)
S III	–	–		6.40	±0.15	(7)
Fe III*	–	–		6.63	±0.23	(4)

The spectral types of NGC 346-11 and AV 304 have been obtained from Rolleston et al. (1993) and the SIMBAD database, operated at CDS, Strasbourg, France respectively.

3.2.1. Effective temperature, T_{eff}

The Si III to Si IV ionization equilibrium was used for estimating the effective temperature and the adopted values are listed in Table 2. Using the grid of models with an iron abundance of 6.4 dex changed these estimates by less than 500 K and hence the adopted model metallicity is unlikely to be a serious source of error. The errors due to uncertainties in the observational data are estimated to be about ±1000 K, whilst those due to the adopted atomic data and physical assumptions are difficult to quantify. However Dufton et al. (2005) discussed the the analysis of two SMC B-type supergiants using the current grids and the unified code FASTWIND (Santolaya-Rey et al. 1997) and found encouraging agreement. Additionally for NGC 346-11, the He II spectrum could be observed and provided an independent estimator. This implied an effective temperature of approximately 33 500 K, which is consistent within the uncertainties in the temperature deduced from the silicon lines (see Fig. 2).

The only other element in which we see two ionization stages is carbon and hence the ionization equilibrium of C II to C III may also be used to deduce T_{eff}. From Table 2 it can be seen that the carbon abundances derived from each species are in excellent agreement for NGC 346-11 but the abundances differ by 0.3 dex for AV 304. Using the C II to C III ionization equilibrium to derive the effective temperature for AV 304 would result in a temperature of 28 300 K which is within the uncertainity and hence consistent with the Si III to Si IV ionization equilibrium temperature.

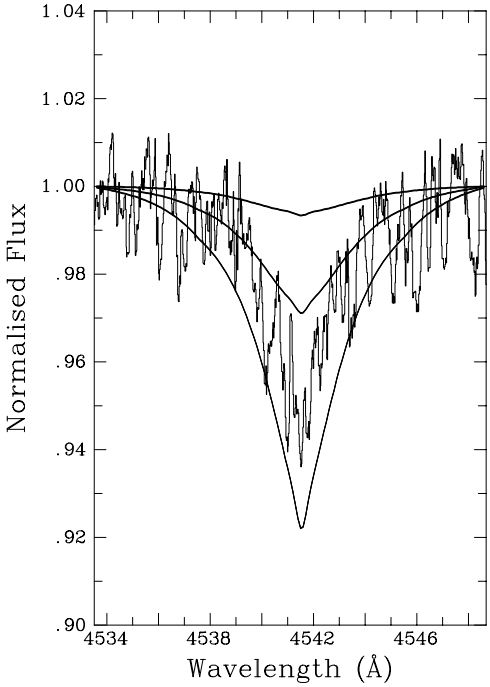

Fig. 2. Observed and theoretical spectra for the He II line at 4541 Å in NGC 346-11. The latter are for effective temperatures of 30 000 K, 32 500 K and 35 000 K (*upper, middle and lower* smooth curves respectively) and imply an estimate of approximately 33 500 K.

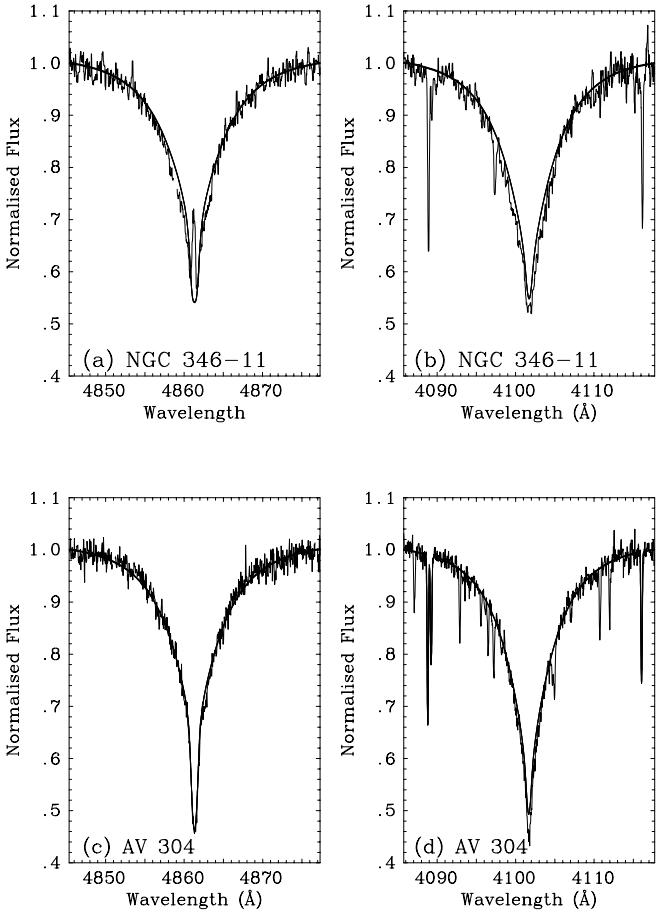

Fig. 3. Examples of the agreement between observed and theoretical (generated using the atmospheric parameters listed in Table 2) Balmer line profiles.

3.2.2. Logarithmic surface gravity, log *g*

Surface gravity estimates were determined by fitting the observed Balmer series lines (Hβ, Hγ and Hδ) with theoretical profiles, with agreement between the different estimates being excellent. The adopted values are listed in Table 2. Observational and fitting errors imply an uncertainty of ±0.1−0.2 dex, whilst an error of 1000 K in the effective temperature would introduce an additional uncertainty of approximately 0.1 dex. As for the estimation of the effective temperatures, the use of the grid with an iron abundance of 6.4 dex yielded similar gravity estimates. The quality of the agreement between observation and theory is illustrated in Fig. 3 for both NGC 346-11 and AV 304. The He II line presented in Fig. 2 can also be used to estimate log g for NGC 346-11. This line implied a value of 4.1 dex which is well within our uncertainity and given the sensitivity of this measurement to our adopted effective temperature we have no reason to believe that this value is more appropiate than that given in Table 2.

3.2.3. Microturbulence, ξ

The microturbulence, as in other studies (see for example Vrancken et al. 2000, and Trundle et al. 2004), proved to be a difficult quantity to determine accurately. The standard technique of eliminating the dependence of the estimated abundance on the line strength (see for example Korn et al. 2000) was used for the O II or Si III spectra. The large number of O II spectral lines should lead to robust estimates of ξ, but the validity of this method may be compromised by the O II lines arising from different multiplets. For the Si III multiplet at 4560 Å, this complication is removed but we are now reduced to only using three lines for the evaluation of ξ.

From the O II lines in AV 304, a value of ξ of 3 km s^{-1} was estimated. By contrast a microturbulence of 1 km s^{-1} was implied by the Si III multiplet. We have adopted a microturbulence in AV 304 of 3 ± 3 km s^{-1} to allow for the uncertainty in this parameter. It should be noted that this uncertainty does not have a significant effect on the other atmospheric parameters.

NGC 346-11 has a higher effective temperature and the metal absorption lines are generally weaker. Indeed for the O II lines, the small range of equivalent widths precluded a reliable estimate of the microturbulence. The Si III lines yielded an estimate for ξ of 5 km s^{-1} but it is not possible to rule out higher values and an uncertainty of ±5 km s^{-1} was therefore adopted. Fortunately the weakness of the metal line spectrum in this star leads to the abundance estimates being relatively insensitive to this quantity and again this uncertainty does not have a significant effect on the other atmospheric parameters.

3.2.4. Projected rotational velocity, $v \sin i$

Both NGC 346-11 and AV 304 are known to have very low projected rotational velocities since the metal lines appear sharp in their spectra. Rotational velocities can be estimated for each

star by rotationally broadening the theoretical spectra, using the procedures discussed in Gray (1992), until they match the observed spectra. Six strong, well defined oxygen and silicon lines were considered, with the theoretical spectra being taken from our non-LTE grid. A projected rotational velocity, $v \sin i$, of 8.0 ± 2.0 km s^{-1} was deduced for NGC 346-11 with the uncertainty being the 1σ standard deviation of the individual estimates. The theoretical spectra for AV 304 at a microturbulence of 3 km s^{-1} is of a similar width to that of the observed spectra and as such any estimate will be highly dependent on the mircoturbulence adopted. Hence, it is not possible to reliably estimate $v \sin i$ although it is clear that it is very low and the observed spectra is dominated by the instrumental resolution. The very low projected rotational velocities make NGC 346-11 and AV 304 ideal for estimating their chemical compositions. However if they indeed have small rotational velocities rather than small angles of inclination, it is possible that they are not representative of the (near) main sequence hot star populations of the SMC.

3.3. Non-LTE photospheric abundances

Non-LTE photospheric abundance estimates were derived for NGC 346-11 and AV 304 using the stellar parameters discussed in Sect. 3.2 and are listed in Table 2. The standard logarithmic scale for presenting abundance estimates has been adopted, where hydrogen is taken to have an abundance of 12.0 dex and all the abundances are relative to this value. The abundances derived from each line in both stars can be found in Table 1.

The uncertainties listed for the photospheric abundances in Table 2 are calculated in two parts. The first considers the random errors associated with analysing the data, e.g. observational uncertainties, individual errors in oscillator strengths etc. This error is taken to be the standard deviation of the derived abundances in each species divided by the square root of the number of absorption lines observed. In cases where only one line of a species was observed, random errors were considered to be equal to the standard deviation of the most observed species (O II) but given that in most cases the systematic errors are larger than the random errors, this assumption should not be critical. The second part considers systematic errors arising from the stellar atmospheric parameter estimates. All the stellar parameters were increased in turn by their uncertainty and the mean abundance derived was compared to the absolute abundance listed in Table 2. In Table 3 we have listed the uncertainties in our abundance estimates due to both the uncertainty arising from random errors and to the uncertainties in the adopted atmospheric parameters.

The total uncertainty in an abundance estimate for a given species was taken as the square root of the sum of the squares of the uncertainty arising from the random errors and the systematic errors arising from the temperature, gravity and microturbulence estimates. In the majority of cases decreasing each of the stellar parameters in turn by their associated uncertainty leads to the same uncertainty as increasing each of the stellar parameters. In cases where there was asymmetry, the uncertainty was taken as the average from increasing and decreasing each of the stellar parameters.

Table 3. A breakdown of the uncertainities in the abundance of each species due to both the uncertainity arising from random errors and the uncertainity in each of the adopted atmospheric parameters.

Species	NGC 346-11				AV 304			
	$\sigma_{\rm obs}$	$\sigma_{\rm T}$	$\sigma_{\rm g}$	σ_{ξ}	$\sigma_{\rm obs}$	$\sigma_{\rm T}$	$\sigma_{\rm g}$	σ_{ξ}
C II	0.17	0.21	0.11	0.03	0.05	0.10	0.04	0.00
C III	0.04	0.10	0.09	0.11	0.01	0.23	0.18	0.06
N II	0.22	0.19	0.09	0.04	0.14	0.11	0.04	0.01
O II	0.05	0.17	0.09	0.01	0.02	0.06	0.02	0.07
Mg II	0.22	0.05	0.01	0.04	0.14	0.06	0.02	0.04
Si III	0.01	0.20	0.04	0.15	0.05	0.08	0.01	0.16
Si IV	0.12	0.10	0.15	0.16	0.09	0.28	0.26	0.19
Ne II	–	–	–	–	0.05	0.12	0.09	0.03
Al III	–	–	–	–	0.06	0.09	0.03	0.02
S III	–	–	–	–	0.12	0.00	0.07	0.06
Fe III	–	–	–	–	0.18	0.14	0.01	0.02

$\sigma_{\rm obs}$ is the standard deviation in the abundances of a given species divided by the number of observed lines; $\sigma_{\rm T}$ is the systematic uncertainity in the abundance given an uncertainity in $T_{\rm eff}$ of $\pm$1000 K; $\sigma_{\rm g}$ is the systematic uncertainity in the abundance given an uncertainity in $\log g$ of $\pm$0.2 dex; σ_{ξ} is the systematic uncertainity in the abundance given an uncertainity in ξ of $\pm$5 km s^{-1}; Note that $\sigma_{\rm obs}$ for N II and Mg II is taken as the standard deviation of the O II abundances.

3.4. Other abundance estimates

As discussed by Rolleston et al. (2003), lines arising from Ne II, Al III, and Fe III were also observed in the spectrum of AV 304 and these species are not currently available in our non-LTE grids. For completeness, we have calculated non-LTE models at the atmospheric parameters listed in Table 2. These have then be used to derive abundance estimates (and uncertainties using the methodology outlined in Sect. 3.3) in an LTE approximation and these values are also listed in Table 2. Note that as we have used effectively the same methods, there is no apriori reason to believe that these estimates are superior to those deduced by Rolleston et al. (2003).

Although sulphur was included in our non-LTE calculations, no grids of S III equivalent widths were calculated. However we have used the models discussed above to generate theoretical non-LTE S III equivalent widths and hence S abundance estimates. It is found that our mean LTE abundance is only 0.01 dex lower than the non-LTE value quoted in Table 2 and hence non-LTE effects appear to be negligible for this species at the atmospheric parameters of AV 304.

For other species, the main non-LTE effect may consist of overionization relative to LTE, but if we use the lines of the dominant ion the LTE abundances will generally be in good agreement with non-LTE abundances. At the atmospheric parameters of AV 304 Fe IV is the dominant species of iron and as such our LTE abundance derived from the Fe III lines is likely to underestimate the actual iron abundance in the SMC.

Article published by EDP Sciences and available at http://www.edpsciences.org/aa or http://dx.doi.org/10.1051/0004-6361:20042290

3.5. Comparison with previous analyses

Rolleston et al. (2003) have previously presented an LTE analysis for AV 304 based on the same observational dataset. They deduced similar atmospheric parameters with a slightly lower surface gravity and higher microturbulence. However, within the estimated uncertainties the two analyses are in agreement. The photospheric abundances are also in reasonable agreement although there are differences ranging up to 0.3 dex. These are probably principally due to non-LTE effects and Lennon et al. (2003) discussed and tried to quantify these effects. They report abundance estimates corrected for non-LTE effects of 7.41, 6.55 and 8.16 dex for the CNO elements respectively. These are in excellent agreement with our results for AV 304 indicating that for these elements, the differences between our results and those of Rolleston et al. (2003) arise from non-LTE effects. The remainder of the species for which we have used non-LTE methods (Mg, Si and S) are in excellent agreement with the abundances reported by Rolleston et al. (2003) and non-LTE effects are thought to be small for these species. For example, Trundle et al. (2004) report non-LTE corrections for the Mg and Si abundances given in Rolleston et al. (2003) to be approximately 0.05 dex for both species.

Additionally Rolleston et al. (1993) undertook an LTE analysis of lower quality AAT/IPCS spectroscopy for both AV 304 and NGC 346-11. They deduced relatively similar atmospheric parameters but with lower effective temperatures. The quality of their spectra limited the number of ionic species that they could identify but for O II in AV 304 and C III in NGC 346-11 agreement with the current analysis is good. For other species differences range from 0.2 to 0.4 dex and given the improvements both in the quality of the observational data and in the theoretical methods, we believe that the values presented here are more reliable.

3.6. Interstellar lines

A similar analysis to that discussed by Rolleston et al. (2003) for AV 304 was used to estimate the LSR velocities of the individual components of the interstellar Ca II K line in NGC 346-11. The velocity of the different components (rounded to the nearest km s^{-1}) are tabulated in Table 4 and illustrated in Fig. 4, with the results for AV 304 being taken directly from Rolleston et al. (2003).

NGC 346-11 shows fewer individual components, possibly due to the larger slit width (and hence lower spectral resolution) used in its observations. Following similar methods to Rolleston et al. (2003) we associate components N1 and N2, along with components A1 through to A4 with our Galaxy. We believe that the remaining components belong to the SMC. From the distinct differences in the profiles, we may be observing different SMC gas components although it is possible to identify interstellar components towards the two stars with similar velocities (for example, 156−157 km s^{-1} and 200−201 km s^{-1}). The targets have an angular separation of 0.53°, corresponding to approximately 500 pc for a distance modulus of 18.89 (Harries et al. 2003). Hence it is not clear whether these components are related although Wayte (1990) identified components that had large spatial extents across both the SMC and LMC.

Table 4. LSR velocities (rounded to the nearest km s^{-1}) of the different components observed in the interstellar Ca II K line. The values for AV 304 have been taken directly from Rolleston et al. (2003).

NGC 346-11		AV 304	
Component	v_{lsr} (km s^{-1})	Component	v_{lsr} (km s^{-1})
N 1	2	A 1	-5
N 2	75	A 2	13
N 3	92	A 3	44
N 4	119	A 4	64
N 5	140	A 5	92
N 6	156	A 6	110
N 7	201	A 7	122
		A 8	136
		A 9	157
		A 10	171
		A 11	187
		A 12	200

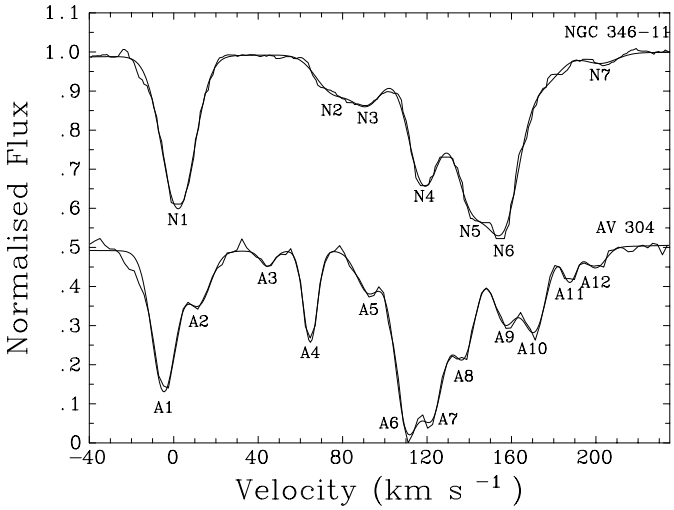

Fig. 4. The observed interstellar gas components towards NGC 346-11 and AV 304, together with the Gaussian fits used to deduce the velocities listed in Table 4.

4. Chemical composition of the SMC

Table 5 presents our best estimate for the present-day chemical composition of the SMC as derived from the photospheric abundances of NGC 346-11 and AV 304. In the following subsections we discuss in detail the methods used to derive these results from the individual abundances listed in Table 2.

4.1. Carbon

The carbon abundance was derived by taking the average of the abundance estimates from C II and C III in each star weighted by the inverse square of their estimated uncertainties. An alternative approach would have been to only use the values showing the lowest uncertainities, viz. the C III abundance from NGC 346-11 and the C II abundance from AV 304. As the

Table 5. Present-day chemical composition of the SMC as derived from NGC 346-11 and AV 304. Also included are the results from some recent studies of B-type stars, viz. Korn et al. (2000) and Trundle et al. (2004) and H II regions in the SMC, viz. Kurt et al. (1999); Reyes (1999); Testor (2001).

	B-type stars			H II regions		
	This paper	Korn et al.	Trundle et al.	Kurt et al.	Reyes	Testor
C	7.42	7.40	7.30	7.53	7.39	–
N	6.55	7.25	7.67	6.59	6.55	6.64
O	8.07	8.15	8.14	8.05	7.96	8.00
Mg	6.77	6.78	6.78	–	–	–
Si	6.64	6.84	6.74	6.70	–	–
Ne	7.84	–	–	7.26	7.17	7.23
Al	5.33	5.58	–	–	–	–
S	6.40	–	–	6.42	6.32	6.31
Fe	6.63	6.82	–	–	–	–

abundance estimates agree relatively well, it is not critical which method we adopt. The former method was used to maintain consistency with the rest of the analysis but using the latter resulted in an absolute abundance only 0.04 dex lower.

4.2. Nitrogen

The nitrogen abundance estimated from the 3995 Å line in the spectra of NGC 346-11 should probably be treated as an upper limit as this weak line is poorly observed in our spectrum. For this reason we have adopted the AV 304 abundance of nitrogen as the nitrogen abundance in the SMC. If the NGC 346-11 result had also been included, the resultant estimate, considering the errors would have been only 0.05 dex higher than the value listed in Table 5.

4.3. Oxygen

Using the same method as discussed for carbon the SMC oxygen abundance was derived. We note that the value deduced for the two stars differ by 0.3 dex and it is unclear whether this represents a real difference or is due to uncertainties in, for example, the estimation of the atmospheric parameters, the different sets of lines used for the two stars or the adopted model ions. To investigate this we have undertaken differential analyses with respect to two Galactic B-type stars, viz. HR 2387 and τ Sco. The former has atmospheric parameters ($T_{\rm eff}$ = 25 500 K; $\log g$ = 3.8; ξ = 5 km s^{-1}) similar to AV 304, whilst those of the latter ($T_{\rm eff}$ = 30 500 K; $\log g$ = 4.2; ξ = 5 km s^{-1}) are similar to NGC 346-11. The differential abundances are then -0.57 ± 0.09 for 30 lines in AV 304 and -0.70 ± 0.09 for 16 lines in NGC 346-11. Hence although there remains a discrepancy, this is significantly reduced, indicating that it probably does not represent a real difference in the stellar O abundances.

4.4. Magnesium

The derived magnesium abundance from each star was the same and the value has been directly transferred into Table 5.

4.5. Silicon

Silicon is the only element where our choice of method for the combination of the abundances derived from the individual species in each star becomes important. The abundance estimates for AV 304 are 0.34 dex higher for both Si III and Si IV compared to the values derived for NGC 346-11. If we adopt the same method to combine the results as was used for the other elements, a value of 6.60 dex would be obtained. However the errors associated with the estimates for NGC 346-11 are dominated by the uncertainty in the adopted microturbulence particularly for the relatively strong Si IV lines. Indeed if a zero microturbulence was adopted, the silicon abundance estimate for NGC 346-11 would increase to 6.60 ± 0.15 dex. Additionally one could argue that the Si IV lines in AV 304 should not be used as these lines are sensitive to changes in the stellar parameters and especially the effective temperature. Hence we have opted to use only the Si III lines using the same weighting as for the other ions. We note that this value is only 0.04 dex higher than that obtained by considering both ionic species. We also note that a differential analysis similar to that descibed in Sect. 4.3 leads to values of -0.74 ± 0.03 (from three lines) for AV 304 and -0.98 ± 0.09 (from six lines) for NGC 346-11, which as for oxygen leads to a decrease in the discrepancy between the two stars although it still remains significant. It is unclear if this represents a real discrepancy or is an effect of the high sensitivity of the Si lines to the stellar parameters.

4.6. Other elements

Lines of other elements were only observed in the spectra of AV 304, and the abundances in Table 5 come directly from those derived for this star and listed in Table 2. For neon, aluminium and iron, these should be treated with caution given the limited number of features observed and the neglect of non-LTE effects.

Dufton et al. (1986) found that non-LTE effects in Al III were relatively small and hence the abundance estimate for this species may be reliable. For S III, there are a relatively large number of well observed features and the uncertainty attached to the mean abundance is relatively small, reflecting in part the good agreement between the abundance estimates and hence this value should also be reliable. For both Ne II and Fe III, the agreement between the estimates from individual lines is relatively poor and these results may be unreliable with the iron value possibly being an underestimated, see Sect. 3.4. Additionally, adopting this value leads to an iron abundance that is approximately 0.3 dex lower than that used in the SMC grid. However as discussed above, the use of models with a lower Fe abundance leads to similar results.

5. Comparison with other SMC B-type stellar and H II region studies

In Table 5 we also present a comparison of our best estimate for SMC abundances with those from other studies of B-type stars and of H II regions. For the former we have included the

non-LTE analysis using static atmospheres of Korn et al. (2000) and the non-LTE unified model atmosphere analysis of Trundle et al. (2004). The three stars analysed by Korn et al. (2000) have logarithmic gravities in the range 2.67 to 2.93 dex and although described by Korn et al. (2000) as "non-supergiants", they have clearly evolved away from the main sequence. The targets of Trundle et al. (2004) are mostly Ia type supergiants with gravities in the range 1.7 to 3.1 dex. There are numerous analyses of H II regions in the SMC including Russell & Dopita (1992), Reyes(1999), Garnett (1999), Kurt et al. (1999), Peimbert et al. (2000) and Testor (2001). Their abundance estimates are generally in quite good agreement and we have therefore listed three representative analyses in Table 5.

Sofia & Meyer (2001) suggest that B-type stars may actually underestimate the chemical composition of the ISM of the Galaxy and that young F and G-type stars may better represent the ISM. Given the good agreement of our stellar analysis with analyses of H II regions there is no evidence that B-type stars underestimate the chemical composition of the ISM in the lower metallicity environment of the SMC, although this possibility cannot be completely discounted.

5.1. Carbon, nitrogen and oxygen

The carbon and oxygen abundance estimates for the three stellar studies are in good agreement, whilst the nitrogen estimates for the evolved stars are significantly higher than that found here. As discussed by both Korn et al. (2000) and Trundle et al. (2004), this probably reflects mixing of nucleosynthetic material to the surface of the evolved stars. Confirmation of this is provided by the excellent agreement between our nitrogen abundance estimate and that found in the H II regions studies. As the inital nitrogen abundance is much lower than those of carbon or oxygen it only requires the processing of a relatively small amount of these elements into nitrogen to produce a significant fractional increase in the nitrogen abundance in the atmospheres of evolved stars (Rolleston et al. 2003). For example, Trundle et al. (2004) and Dufton et al. (2005) have found nitrogen enhancements of approximately 1.0 dex in SMC supergiants. However, as discussed by these authors, the evolutionary models of Maeder & Meynet (2001) would imply relatively small corresponding C depletions (<0.25 dex). This is consistent with the near normal C abundances found in SMC supergiants.

Our carbon and oxygen abundance estimates are also in good agreement with the H II region studies and should probably be preferred over the other B-type studies as they are less likely to be affected by small amounts of mixing of nucleosynthetic material to the surface. Heap et al. (2004) have derived abundances from 17 O-type stars in the SMC and these are in excellent agreement with our abundance estimates for cabon and oxygen. From their three targets that do not appear to show enhanced nitrogen they derive a nitrogen abundance 0.15 dex lower than that given here. This may not be significant given the errors in our estimate and the weakness of the N II spectrum in our targets.

5.2. Magnesium and silicon

All the B-type stellar studies yield very similar Mg values probably reflecting the relatively simple term structure for this ion and small non-LTE effects found for B-type stars (see, for example, Mihalas 1972). No comparison was possible with the H II region studies but our estimate is in excellent agreement with that deduced for A-type (Venn 1999; 6.82 dex) and for late-type (see, for example, Spite et al. 1989, 1991; 6.79 dex) stars. The silicon abundance derived here should be treated with some caution given the difference in our estimates for our two targets. Nevertheless, our reported value agrees well (within our uncertainties) with the B-type supergiant value of Trundle et al. and the H II region value of Kurt et al. It is also in agreement with the late-type stellar value of Spite et al. (1989, 1991; 6.75 dex) but is lower than the B-type estimate of Korn et al. and the A-type estimate of Venn (1999; 6.97 dex). Our silicon abundance is also in reasonable agreement with the value derived from O-type stars (Heap et al. 2004; 6.85 dex).

5.3. Neon, aluminium, sulphur and iron

As discussed above the estimates for neon, aluminium and iron are based on LTE calculations and hence may be less reliable. For aluminium and iron, our estimates are in reasonable agreement with the B-type stellar study of Korn et al. (2000), although we find a relatively poor agreement between the values deduced from individual features of iron. Additionally, the B-type estimates for iron are lower than those found in A-type (Venn 1999; 6.70 dex) and late-type (Spite et al. 1989, 1991; 6.72 dex) stars. Peters & Adelman (2002) have derived an iron abundance for AV 304 from Far Ultraviloet Spectroscopic Explorer (FUSE) data which is 0.2 dex higher than our value although considering the uncertainity in the estimate this may not be significant. We are also able to compare our iron abundance to that derived from O stars by Bouret et al. (2003) and Heap et al. (2004) and our estimate is again lower than the values derived therein. It is therefore possible that our iron abundance is underestimated due to Fe III not being the dominant ionization stage as discussed in Sect. 3.4.

For neon, our estimate is significantly larger than those found from H II region studies. Given the spread of values estimated from the three stellar features and the lack of any non-LTE calculations for this element, the latter should be considered more reliable. By contrast our sulphur abundance estimate is based on a relatively large number of features that show reasonable internal agreement. Additionally, it is in excellent agreement with the H II region studies and as it has been treated using non-LTE methods it should be considered as reliable, although it is lower than the O-type stellar results of Heap et al. (2004).

6. Conclusions

The principle aim of this analysis was to provide abundance estimates for two unevolved B-type stars in the SMC. These should be representative of their progenitor interstellar material and as such should complement those deduced from

H II region studies. Additionally the high quality of the observational material (coupled with the small stellar projected rotational velocities) and the use of non-LTE model atmosphere techniques should lead to more reliable estimates than have previously been deduced from main sequence SMC targets. For the ions included in the non-LTE calculations, our estimates for C, N, O, Mg and S should be reliable with that for Si being slightly more uncertain. It is difficult to quantify the uncertainties in these values and in particular those arising from the physical assumptions adopted. However from our estimated uncertainties and from a comparison with other studies, we believe that these estimates should normally be accurate to ±0.2 dex or better. For the ions considered in an LTE approximation, the estimates for Al may be reliable, whilst those for Ne and Fe should be treated with caution.

Assuming that the SMC is well mixed, these estimates provide the best estimates of the chemical composition of the SMC as available from unevolved B-type stars. As such they will be particularly useful in interpreting the results from studies of other, possibly evolved, B-type stars, which have utilised similar methods.

Acknowledgements. We are grateful to the staff of the European Southern Observatory for help obtaining the observational data. RSIR and WRJR acknowledges financial support from PPARC (grant No. G/O/2001/00173), D.J.L. acknowledges support through QUB's visiting fellow programme (grant No. V/O/2000/00479).

References

Barbuy, B., Spite, M., Spite, F., & Milone, A. 1991, A&A, 247, 15
Bouret, J.-C., Lanz, T., Hillier, D. J., et al. 2003, ApJ, 595, 1182
Cioni, M.-R. L., & Habing, H. J. 2003, A&A, 402, 133
D'Odorico, S., Cristiani, S., Dekker, H., et al. 2000, in SPIE 4005 Conf., 121
Dufton, P. L., Brown, P. J. F., Lennon, D. J., & Lynas-Gray, A. E. 1986, MNRAS, 222, 713
Dufton, P. L., Fitzsimmons, A., & Howarth, I. D. 1990, ApJ, 362, L59
Dufton, P. L., Ryans, R. S. I., Trundle, C., et al. 2005, A&A, in press
Evans, C. J., Howarth, I. D., Irwin, M. J., et al. 2004, MNRAS, submitted
Gardiner, L. T., & Noguchi, M. 2003, MNRAS, 278, 191
Garnett, D. R. 1999, IAU Symp., 190, 266
Gray, D. F. 1992, The observation and analysis of stellar photospheres (Cambridge: Cambridge Univ. Press)
Harries, T. J., Hilditch, R. W., & Howarth I. D. 2003, MNRAS, 339, 157
Harris, J., & Zaritsky, D. 2004, AJ, 127, 1531
Heap, S. R., Lanz, T., & Hubeny, I. 2004, ApJ, submitted
Hill, V. 1997, A&A, 324, 435
Hill, V. 1999, A&A, 345, 430
Howarth, I. D., Murray J., & Mills D. 1994, Starlink User Note, No. 50.15
Hubeny, I. 1988, Comp. Phys. Comm., 52, 103
Hubeny, I., Heap, S. R., & Lanz, T. 1998, in Boulder-Munich: Properties of Hot, Luminous Stars, ed. I. D. Howarth, ASP Conf. Ser., 131, 108
Hubeny, I., & Lanz, T. 1995, ApJ, 439, 875
Kilian, J. 1992, A&A, 262, 171
Kilian, J., Montenbruch, O., & Nissen, P. E. 1994, A&A, 284, 37
Kim, S., Staveley-Smith, L., & Dopita, M. A. 2003, ApJS, 148, 473
Korn, A. J., Becker, S. R., Gummersbach, C. A., & Wolf B. 2000, A&A, 353, 655
Korn A. J., Keller, S. C., Kaufer, A., et al. 2002, A&A, 385, 143
Kunkel, W. E., Demers, S., & Irwin, M. J. 1995, Proc. Third CTIO/ESO Workshop, The Local Group: Comparatives and Local Properties (ESO, Garching), 200
Kurt, C. M., Dufour, R. J., Garnett, D. R., et al. 1999, ApJ, 518, 246
Lennon, D. J., Dufton, P. L., & Crowley, C. 2003, A&A, 317, 87
Maeder, A., & Meynet, G., 2001, A&A, 373, 555
McErlean, N. D., Lennon, D. J., & Dufton, P. L. 1999, A&A, 349, 553
Mihalas, D. 1972, ApJ, 177, 115
Peimbert, M., Peimbert, A., & Ruiz, M. T. 2000, ApJ, 541, 688
Peters, G. J., & Adelman, S. J. 2002, A&AS, 201, 113
Reyes, C. 1999, IAU Symp., 190, 282
Rolleston, W. R. J., Dufton, P. L., Fitzsimmons, A., Howarth, I. D., & Irwin, M. J. 1993, A&A, 277, 10
Rolleston, W. R. J., Venn, K., Tolstoy, E., & Dufton, P. L. 2003, A&A, 400, 21
Russell, S. C., & Dopita, M. A. 1992, ApJ, 384, 508
Ryans, R. S. I., Dufton, P. L., Mooney, C. J., et al. 2003, A&A, 401, 1119
Santolaya-Rey, A. E., Puls, J., & Herrero, A. 1997, A&A, 323, 488
Sofia, U. J., & Meyer, D. M. 2001, ApJ, 554, 221
Spite, M., Barbury, B., & Spite, F. 1989, A&A, 222, 35
Spite, F., Richtler, T., & Spite, M. 1991, A&A, 252, 557
Stanimirovic, S., Staveley-Smith, L., & Jones, P. A. 2004, ApJ, 604, 176
Testor, G. 2001, A&A, 372, 667
Trundle, C., Lennon, D. J., Puls, J., & Dufton, P. L. 2004, A&A, 417, 217
Venn, K. A. 1999, ApJ, 518, 405
Vrancken, M., Lennon, D. J., Dufton, P. L., & Lambert, D. L. 2000, A&A, 358, 639
Wayte, S. R. 1990, ApJ, 355, 473
Welty, D. E., Frisch, P. C., Sonneborn, G., & York, D. G. 1999, ApJ, 512, 636
Welty, D. E., Lauroesch, J. T., Blades, J. C., et al. 1997, ApJ, 489, 672
Westerlund, B. 1997, in The Magellanic Clouds (Cambridge University Press)
Yoshizawa, A. M., & Noguchi, M. 2003, MNRAS, 339, 1135
Zaritsky, D., & Harris, J. 2004, AJ, 604, 167

Online Material

Article published by EDP Sciences and available at http://www.edpsciences.org/aa or http://dx.doi.org/10.1051/0004-6361:20042290

Table 1. The equivalent widths (*EW*) and derived abundances for the metal lines observed in the spectra of AV 304 and NGC 346-11.

		AV 304		NGC 346-11	
Species	Wavelength Å	*EW* mÅ	Abund.	*EW* mÅ	Abund.
C II	3919.0	13	7.46	–	–
C II	3920.7	17	7.34	7	7.62
C II	4267	55	7.29	21	7.28
C III	4647.4	48	7.67	83	7.40
C III	4651	55	7.65	110	7.48
N II	3995	16	6.55	8	6.73
O II	3851	11	7.72	–	–
O II	3857	11	8.05	–	–
O II	3864	38	8.01	–	–
O II	3912	52	8.08	17	7.81
O II	3919.3	34	8.15	–	–
O II	3945.0	36	8.19	–	–
O II	3954.4	54	8.14	14	7.76
O II	3982.7	34	8.19	–	–
O II	4069	125	8.13	54	7.81
O II	4072.2	78	7.99	41	7.75
O II	4075.9	86	7.91	38	7.54
O II	4078.8	32	8.16	–	–
O II	4132.8	44	8.19	12	7.72
O II	4185.4	42	8.02	9	7.41
O II	4317	61	8.23	16	7.95
O II	4319.6	67	8.32	16	7.96
O II	4325.8	26	8.45	–	–
O II	4349.4	95	8.34	45	8.22
O II	4351	64	7.94	–	–
O II	4366	64	8.21	27	8.12
O II	4369.3	17	8.11	–	–
O II	4414.9	93	8.13	22	7.77
O II	4417.0	77	8.24	12	7.72
O II	4443.0	15	8.09	–	–
O II	4452.4	33	8.34	–	–
O II	4591.0	67	8.05	17	7.60
O II	4596.2	59	8.05	12	7.54
O II	4638.9	71	8.22	23	8.00
O II	4641.8	95	8.06	46	7.99
O II	4650	181	8.07	77	7.92
O II	4661.6	77	8.21	31	8.08
O II	4673.7	22	8.31	–	–
O II	4676.2	62	8.16	27	8.12
O II	4699	58	7.96	–	–
O II	4705.4	55	7.96	12	7.50
O II	4751.3	10	8.15	–	–
O II	4890.9	18	8.09	–	–
O II	4906.8	28	7.99	11	7.81
O II	4924.5	44	8.23	–	–
O II	4941.1	20	8.16	–	–
O II	4943	34	8.22	–	–
O II	4955.8	10	8.28	–	–
Mg II	4481	49	6.77	35	6.77
Si III	3806	42	6.70	–	–
Si III	4552.6	95	6.66	45	6.42
Si III	4567.8	83	6.78	30	6.41
Si III	4574.8	51	6.89	11	6.42
Si IV	4088.9	60	6.64	78	6.15
Si IV	4116.1	49	6.82	74	6.47
Si IV	4212	–	–	16	6.55
Ne II	4391.9	11	7.81	–	–
Ne II	4409.3	10	7.87	–	–
Al III	4529.2	10	5.33	–	–
S III	3860.4	6	5.92	–	–
S III	3983.8	6	6.01	–	–
S III	3986.0	8	6.50	–	–
S III	4253.6	49	6.59	–	–
S III	4285.0	30	6.46	–	–
S III	4361.5	18	6.84	–	–
S III	4364.7	8	6.43	–	–
Fe III	4164.8	7	6.38	–	–
Fe III	4310.4	9	6.75	–	–
Fe III	4419.6	10	6.32	–	–
Fe III	4431.0	7	7.06	–	–

Table 1. continued.

The wavelengths of unresolved blends of lines are quoted to the nearest angstrom. The equivalent widths of the spectral lines in AV 304 have been obtained from Rolleston et al. (2003). The equivalent widths of the spectral lines in NGC 346-11 have been measured using the line fitting program ELF in the spectral analysis package DIPSO (Howarth et al. 1994).

Article published by EDP Sciences and available at http://www.edpsciences.org/aa or http://dx.doi.org/10.1051/0004-6361:20042290